MAGNETIC FIELD EFFECTS ON SUPERCONDUCTING CAVITY

M. Ono#, E. Kako, K. Saito, T. Shishido, S. Noguchi and T. Yokoi, KEK, 1-1, Oho, Tsukuba-shi, Ibaraki-ken, 305-0801, Japan

Abstract

The effects of external magnetic field were experimentally investigated. The surface resistance (R_s) of L-band scc were measured in the following two conditions of external H-field; the parallel fields to the beam axis were applied before and after the superconducting state transition. The increasing of the R_s as a function of H-field was observed in the former condition, and it may be explained by the magnetic flux trapping. The latter test is intending to break the super state by the strong external H-field. The super state breaking may start at below the lower critical field (H_{c1}) owing to the demagnetizing coefficient of the cavity shape. These experiments were motivated by the scc applications at the strong H-field environment.

1 INTRODUCTION

Owing to the good performances of the superconducting cavity and great development of the relevant construction technologies, the application of it for wider area are considered. The feasible study of the application in the strong magnetic field environment is one example; the secondary beam acceleration with strong focusing magnetic field [1]. On the other hand, the magnetic properties of the superconductor itself are quite interesting to explore [2], and experimental studies of these will be also required for getting fundamental information needed in the realization of the applications.

An L-band superconducting cavity (K-14, [3]) made of niobium sheet was used in these experiments; the shape of the cavity and other parameters of its can be found in ref. [3] or in references cited there. It is already known [4] that the magnetic field existed beforehand the superconducting phase-transition contribute to the residual surface resistance. The reconfirmation of this behavior and the discussions about the results are described in section 3 ("Weak magnetic field"). In the later sections (4, 5), the experiments at the "High magnetic field" and their results are described. The high fields of these studies are applied after the phase transition to investigate the super-state braking by the external field. Before describing of these experiments, lower and upper critical field of the niobium are summarized or estimated in the next section 2. The estimations are carried out with using the data that were taken at KEK by one of the authors. In general, the measured values of these are strongly affected by the preparation of the sample pieces. In this sense, using the data taken at KEK may be reasonable even though these are not necessary accepted as the world's standard at this moment. The consistency with other data including the results of this paper, may justify the accepted parameters as discussed in the relevant sections.

2 CRITICAL FIELD

The parameters of niobium that will be used in the following sections are estimated and summarized as follows:

- $H_c(0) = 2060 \pm 50$ Oe : Thermodynamic critical field[5]
- $H_{c1}(0) \approx 1700$-1800 Oe : Lower critical field
- $H_{c2}(0) \approx 2400$-2500 Oe : Upper critical field
- $H_{c3}(0) \approx 4250$ Oe : Surface superconductivity critical field
- $\kappa \approx 0.71$-0.856 , $\sqrt{2}\kappa \approx 1.14$-$1.21$: G-L parameter

The temperature dependence of all the critical fields are assumed as follow.

$$H_c(T) = H_c(0) \times (1 - (T/T_c)^2) \qquad (1)$$

This dependence has been empirically established.

2.1 Estimate H_{c1} and H_{c2} from Sample Data

The H_{c1} measured by one of authors (K. Saito) with using niobium test samples have been reported in reference [6]. The data are shown in figure 1 again. These already indicate that the measured results were much depend on the preparations of the samples. Here we simply adopt the lowest data to estimate H_{c1}, because that effects of a surface condition of the sample may increase the measured values and that a bulk properties may be close to the lowest one, as discussed later. The temperature dependence of these is consistent with equation (1) with $H_{c1}(0) = 1700$ Oe.

About the H_{c2}, no temperature dependence data were reported in ref.[6], but just indicated in figure 13 as an end point of a slowly diminished line. As an experimental method, it is quite difficult to obtain such end point and this method may introduce large ambiguities in the obtained values. Also these end points (≥4000 Oe at 2K) can't be identified as H_{c2} even though large ambiguities are taking into account. Let's take the thermodynamic and lower critical field as $H_c(0) = 2060$ Oe [5] and $H_{c1}(0) = 1700$ Oe. With these values, $H_{c2}(0)$ must be around 2500 Oe, because of a definition of H_c; H_c is an average value

E-mail: onom@post.kek.jp

of H_{c1} and H_{c2} in some sense, actually defined as an equivalent magnetic energy ($\mu_0 H_c^2/2$) equal to the integration of the magnetization up to H_{c2}. For the niobium, it is said that $\sqrt{2}\kappa$ (Ginzburg-Landau parameter) is greater than 1 (type-II) but close to unity. If so, we can expect a relation of $H_c - H_{c1} \approx H_{c2} - H_c$ as order estimation of H_{c2}.

In the following we assume the above end points as H_{c3} instead of H_{c2}. At the external field situation of the sample tests, up to H_{c3} ($>H_{ext}>H_{c2}$) the superconducting state is still remain at the surface region even though the interior area is transited to normal state, and a relation of $H_{c3} \approx 1.7H_{c2}$ is given [2]. Then the lowest data of H_{c3} in figure 1 indicate the values of H_{c2} and κ; $H_c(2K) \approx 4000/1.7 \approx 2350$ Oe, $\sqrt{2}\kappa \approx H_{c2}(2K)/H_c(2K) \approx 1.2$. If we simply assume $H_{c1}=H_c/\sqrt{2}\kappa$ then we can estimate $H_{c1}(2K) = 1620$ Oe, and this is quite consistent with the H_{c1} sample data shown in figure 1.

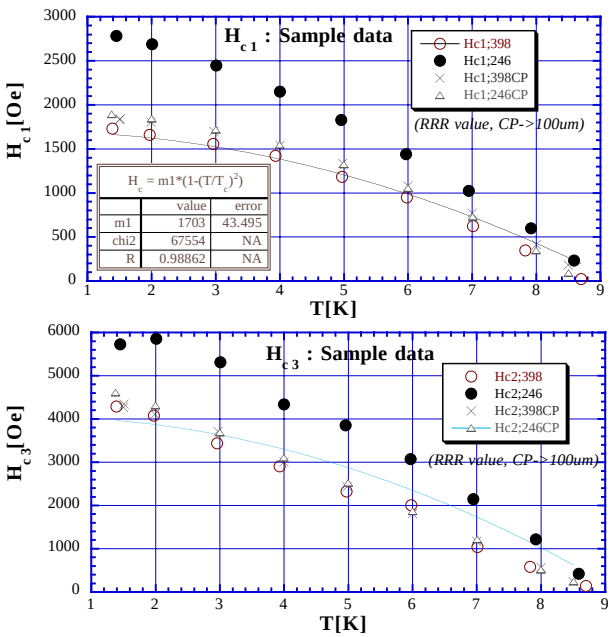

Figure 1: H_{c1} and H_{c3} of sample pieces. See ref.[6]

Several comments are in order. The data (see [6] for sample preparation) indicate that the rather dirty surface sample show the higher H_{c1} or H_{c3}. Because that the H_{c3} is defined at the end point of the diminished line, H_{c3} is corresponding to the disappearance of the final super state, no matter how the partial destruction of super state is already happened. For H_{c1}, shielding by the dirty surface-super-current may increase it. Therefore, the lowest data may indicate the bulk properties. The Ginzburg-Landau theory does not give a simple relation between H_c and H_{c1} for small κ case; the factor $\log\kappa/\sqrt{2}\kappa$ can be applicable for large κ case only. On the other hand, in the relation between H_c and H_{c2} there is no limitation on κ and we use this for deduction of κ.

2.2 Comparison with RF Field

The estimation of H_{c1} is tried with the magnetic field of rf-field. At an accelerating field of E_{acc} = 40 MV/m, the corresponding peak magnetic field at the equator can be calculated; $H_{c1,rf}(1.8K)$ = 1728 Oe, for the parameter H_{sp}/E_{acc} = 43.2 Oe/MV/m of the cavity used in this experiment. Actually this cavity (K-14) attained the first 40MV/m at KEK as reported in reference [3]. If the same temperature dependence of (1) is assumed, $H_{c1,rf}(0) \approx$ 1800 Oe. Because that the H-field and the cavity surface at the equator is almost parallel, a demagnetization coefficient; n_{rf} may be assumed as zero. If very naively we assume that H_{c1} for dc-case is same as rf-case, the corresponding κ and H_{c2} are 0.71 and 2400 Oe, respectively. In this estimation, it is assumed that the limitation of 40MV/m for E_{acc} is come from the excess of the rf magnetic field over the H_{c1}, and that this H_{c1} is same to the static one.

Several comments are expressed here. After this cavity attained the 40MV/m E_{acc}, already 6 cavities in KEK also attained the same level accelerating field but never exceed this level. It seems that the common limitation mechanism is working. The next comment is concerning about the equality of H_{c1} between the rf and the static case. As it will be discussed in subsection 4.3, the cancellation of the trapped vortex lines are not perfect even if the reverse field are applied at the same strength when the pinning effects are exist. If so, the trapped vortex will be partially remained and be accumulated at every rf-cycles and eventually these induce the quench. The superheating critical field, H_{sh} are measured (in pulsed mode) and discussed in ref. [7] with relating to rf field; $H_{sh} \approx 1.2H_c$ for $\kappa \approx 1$. But in these high magnetic fields, the Meissner state is metastable state as similar to the arguments of H_{c3}. Therefore, in the CW operation of the cavity, it may be quite difficult to attain the ideal surface to maintain such metastable state in the actual cavity with the presently available technologies. If so, it may be plausible to assume that the H_{c1} limited the maximum field as we discussed here, because of the bulk property of H_{c1} (see more discussion in 4.3).

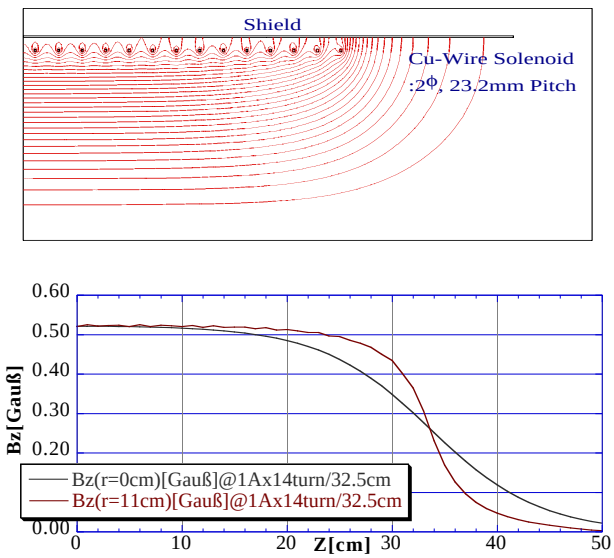

Figure 2: H-field by copper wire solenoid coil. A small ringing of the field is observed at larger radius.

3 WEAK MAGNETIC FIELD

The effects of the magnetic field on the surface resistance of the cavity are experimentally explored. Where the magnetic field was applied beforehand a cooling down of the cavity.

3.1 Experimental Apparatus

A copper wire solenoid coil was set to envelop the cavity in the helium-vessel and it generate the magnetic field in parallel to the beam axis of the cavity at lest at the cavity region. The size of the coil is 650mm long with 260Φ diameter and 28 turns in total. A small field ringing may exist at larger radius as shown in figure 2, but its magnitude is small enough compared to the field uncertainty. The uncertainty mainly comes from the field calibration carried out by using a Hall probe with unshielded condition. The

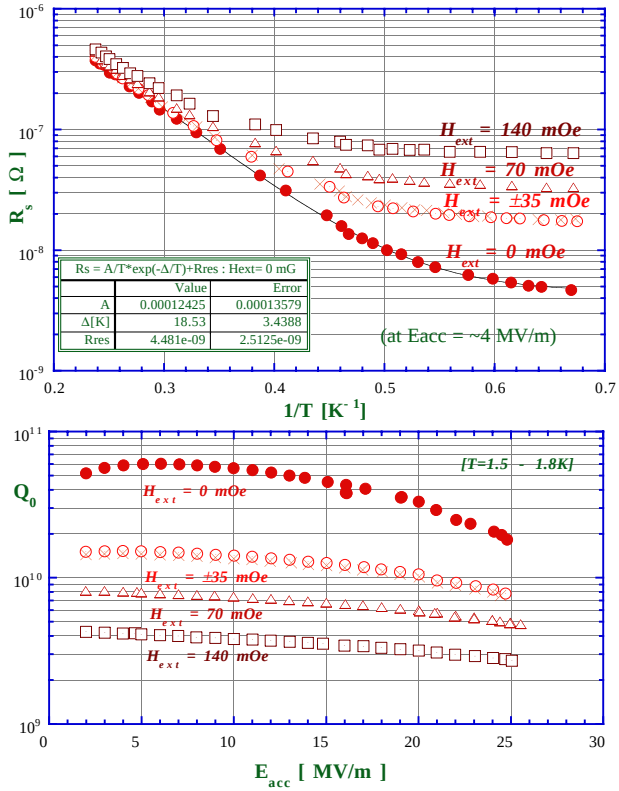

Figure 3: R_s as a function of Temperature, and Q-E curve for each H-fields

simulation code (“Poisson”) tells us the effects of the shield condition up to 7%; unshielded case 7% lower than the shielded condition. The big uncertainty comes from the discrepancy between the ~30% lowered measured value and simulated value. In the following results and discussion of this section, we use the measured values as calibration factors (in the next section we use simulation results instead, because we didn’t calibrate at high field). The data were taken at 0, ±35, 70 and 140mOe external fields. At each field changing, the cavity was wormed up and was cooled down again to measure. During these thermal cycles, the cavity was closed without using any vacuum pump. A cylindrical μ-metal shield for geomagnetism is set inside the cryostat (inner shield). The residual magnetic field in the cryostat is estimated as ~15 mOe by a Hall probe measurement. If we use the results of this section, the data of reverse polarity of this experiment (±35mOe) gives ~1 mOe in the beam axis direction. Also if we assume that all the residual resistance (R_{res}) is comes from the trapped field, then ~8mOe residual field is estimated. In any way, 15±5(?) mOe residual field may be exist.

3.2 Experimental Results

Figure 3 shows the temperature dependence of surface resistance (R_s) and the Q_0-value as a function of accelerating field (E_{acc}). The R_s is expressed as shown in equation (2), and extract a residual surface resistance

(R_{res}) as a temperature independent term. The T-dependent term is called as BCS term.

$$R_s(T) = A/T \exp(-\Delta/T) + R_{res} \qquad (2)$$

To extract R_{res} accurately, the temperature was lowered to ~1.5K. The obtained BCS parameters (A, Δ) of zero H-field

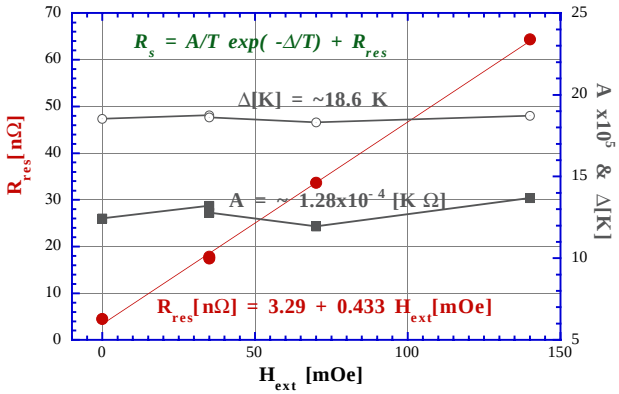

Figure 4: H-field dependence of the parameters; A, Δ, R_{res}

were well reproduced the previous data [3]. The Q-E curve shows no changing the maximum E_{acc} at each H-field, even though the 25MV/m (and Q-degradation at above 15MV/m) is not so good for this cavity if we compare it to 40MV/m that was attained by this cavity before. But no changing of maximum E_{acc} at each H-field may indicate that the surface condition at each thermal cycle wasn't changed, and that the quench mechanism may not be relevant to the applied H-field. So, the changing of R_s at each experiment may come from the effects of the applied H-field.

Figure 4 shows the H-field dependence of the parameters appeared in equation (2). A big effect is observed in R_{res} and expressed as shown in equation (3), while the effect on the BCS parameters (A, Δ) are scarcely observed.

$$R_{res}[n\Omega] = 3.29 + 0.433\, H_{ext}[mOe] \qquad (3)$$

The constant term express the residual H-field effect if all of origins of R_{res} are a flux trapping that is explained in 3.3. Also, its absolute value is affected by the solenoid coil field calibration. The difference between H_{ext} = ±35mOe data is ~0.4nΩ. These informations were used for residual field estimation in the previous subsection.

3.3 Discussion

The interpretation of the H-field dependence of R_{res} (3) is explained [4] as follow. The H-field beforehand existed are trapped in the superconductor as a bundle of the fluxoid (quantized magnetic flux; $\varphi = hc/2e = 2\ 10^{-7}$ gauss cm^2), because of the type-II superconductor; the mixed-state. The central region of the fluxoid is normal state and its size is order of the coherence length (ξ). Then a surface resistance caused by the trapped fluxoid (R_{mag}) may be expressed in terms of normal state surface resistance (R_n) and H-field (H_{ext}) with ξ or H_{c2}; assuming that normal area $\sim\pi(\xi/2)^2$, $H_{c2}=\varphi/2\pi\xi^2$ and fluxoid penetrate double planes for the cavity at the parallel H-field condition to the beam axis.

$$R_{mag} = 2N\pi(\xi/2)^2 R_n = (H_{ext}/H_{c2})\, R_n = H_{ext}\,(R_n/H_{c2}) \qquad (4)$$

Where N is a number of fluxoid per unit area; $H_{ext} = N\varphi$. If

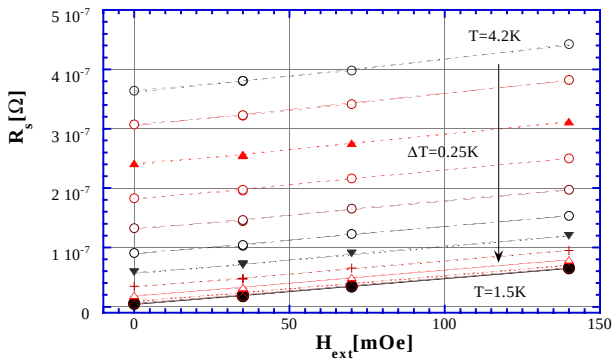

Figure 5: R_s as a function of H_{ext}; slope of each line = α_{slp}

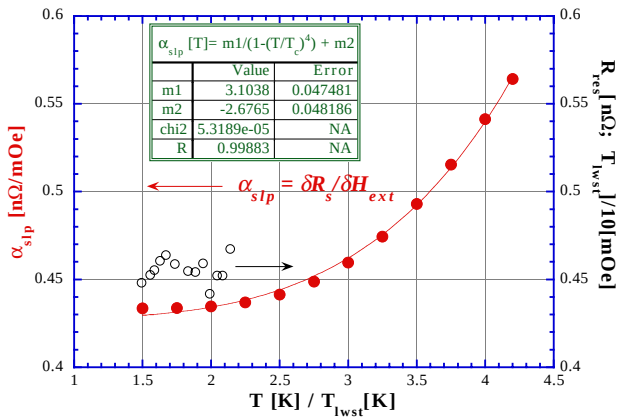

Figure 6: T-dependence of α_{slp}; black. And R_{res}/10mOe deduced from T_{lwst} to 4.2K; white.

we use the value of $H_{c2}(2K) \approx 2350$Oe and $R_n \sim 1$mΩ [10], then $R_n/H_{c2} \approx 0.426$ [nΩ/mOe]. We don't necessary insist that the discussion given above is correct up to the factors, even though the quite good (may be accidental) coincidence with 0.433 of equation (3). Main ambiguities may come from the factor of the definition of normal area of the vortex, the estimated value R_n, and the absolute accuracy of H_{ext} in the experiment; factor 2 uncertainty may be expected in the coefficient.

If we accept the equation (4), R_{mag} should exhibit temperature dependence, because of the T-dependence of ξ or H_{c2}. If we identify the H-field dependent term of R_{res} with R_{mag}, then R_{res} is also should shows the (weak) T-dependence, even though the R_{res} is obtained as T-

independent term in the equation (2). Let's define the slope parameter (the coefficient of H_{ext}) as a function of T.

$$\alpha_{slp} = \delta R_{res}/\delta H_{ext} = \delta R_s/\delta H_{ext} \quad (5)$$

The 2nd equality is comes from that the independence of BCS parameters on H_{ext} as shown in figure 4. Figure 3 already shows that good reproducibility of T-dependence of R_s by the equation (2), therefore the R_s at the same temperature for each H-field can be calculated, and shown in figure 5; the slope of each straight line is α_{slp}.

Figure 6 shows the T-dependence of α_{slp} and this dependence is well fitted to $1/(1 - (T/T_c)^4)$ instead to $1/(1 - (T/T_c)^2)$ which is expected from H_{c2} T-dependence. It seems that the microscopic BCS theory may indicate T^4 dependence through ξ; T-dependence of λ(penetration length) calculated by BCS theory [2] shows $1/(1 - (T/T_c)^4)^{1/2}$, and if $\kappa=\lambda/\xi$ scarcely depend on T (as usually assumed) then ξ^2 show $1/(1 - (T/T_c)^4)$ dependence. In the given T-range, the variance of α_{slp} is so small compared to the BCS term of equation (2), therefore this term can be treated as constant in the practical use. What we insist is, if the arguments given above is correct, T^4 dependence of α_{slp} is one confirmation of the field trapping mechanism; R_{mag} is explained by the vortex and by its structure.

Comment on the appearance of H_{c2} in equation (4). The relation $H_{c2} = \varphi/(2\pi\xi^2)$ is used but this relation is derived from the Ginzburg-Landau equation at higher temperature condition (nonlinear terms of G-L equation can be dropped). Therefore, the contradiction of T-dependence between $\alpha_{slp}(T^4)$ and $H_{c2}(T^2)$ is not the contradiction contained in the arguments; $\xi(T^4)$ is directly related in the vortex structure.

The white data of figure 6 show the $R_{res}/10mOe$ deduced from the fitting procedure to the equation (2) of the figure 3 data (T-dependence of R_{res} at $H_{ext}=0$) but removed the data points whose temperature are less than T_{lwst}. The denominator 10mOe is just chosen as the residual H-field for convenient comparison; we estimated the residual field of this order. The R_{res} for higher T_{lwst} show unreasonable values because of the accuracy of the data, especially small bumped data around the λ-point in the figure 3. Practically, the weak T-dependence observed in α_{slp} can't be obtained in the usual fitting procedure.

4 HIGH MAGNETIC FIELD

4.1 Experimental Apparatus

The strong magnetic fields applied to the cavity in parallel to the beam axis were generated by superconducting solenoid coil. A cylindrical μ-metal shield is set at out of cryostat (outer shield; dia.=800mm). The inner shield used in the weak field experiments is removed for minimizing the interference with other experiments. The field distribution simulated by the code "Poisson" is shown in figure 7, where the cavity is also included as a perfect superconductor. The condensation of the field are occurred at the cavity equator and the ratio of this condensed field to the applied field is ~1/0.611. If this ratio is interpreted by the demagnetization coefficient n_{sim} as follow,

$$1/(1 - n_{sim}) \quad (6)$$

then $n_{sim} \approx 0.39$, because that the cavity acts as a perfect demagnetized material. The same simulation but without the cavity gives the 13.75 Oe/1A field strength at the central region of the coil as the external H-field for 640mm length and 268Φ inner diameter solenoid (the estimated value for infinite length is 14.77 Oe/1A). The field at the cavity occupied region is almost parallel as we intended. The field calibrations at high field were not carried out experimentally, so we simply take the simulation value (13.75 Oe/1A). The uncertainty of this value may be a few % that depend on the shield condition.

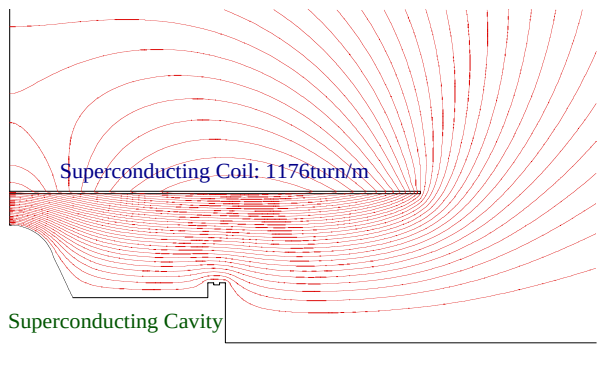

Figure 7: Simulation of H-field with superconducting cavity.

Comment on the H-field at inside the cavity may be required, because that the cap flanges at both sides were made of stainless steel, and an input and a monitor couplers are attached at each side. The H-field applied after the transition can never penetrate into the inside area through both flanges, as far as the zero resistance at outer surface is maintained; this is not the result of Meissner effect, but the result of perfect conductivity. On the other hand, the H-field existed in the cavity inside before the transition will remain after the transition even though the external field is eliminated after the transition, because of Meissner effect (for type-I).

The extra residual magnetic field caused by the outer shield may affected to the data discussed in this section, because that relatively strong field experiments were carried out previously (before success the super-state braking, the coil excitation was failed at ~500Oe, because of a heating at a connection between a copper-wire and SC coil) and the magnetization of the outer shield may be occurred at there. A few nΩ increasing of the surface resistance were observed and these would indicate that the extra field will be ~10mOe (in total 20-30mOe), if we

estimate it by using the 0.433 nΩ/1mOe that is obtained in the previous section. To avoid further magnetization by the further strong fields, alternately polarity changing excitation of the coil have been tried with using bi-polar power supply. Even though it was not clear that these procedures was effective for avoiding the magnetization, it seems that the final residual field was not worsened so much.

4.2 Experimental Result

Figure 8 shows the Q_0 as a function of the applied external magnetic field (H-field) for three cavity temperatures; T=1.4, 2.7 and 4.2K, respectively. The data were taken at E_{acc} = 3-4 MV/m. As already discussed before, the residual field of the outer shield may decreased the Q_0 if we compare it with the previous data of this cavity [3], but these Q-degradation are irrelevant to the purpose of this section.

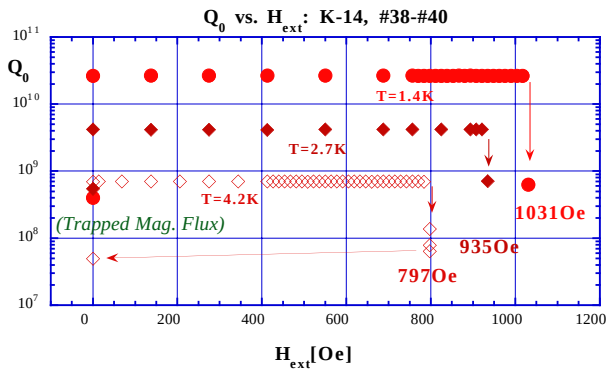

Figure 8: Effects of external H-field: Q_0 vs. H_{ext}

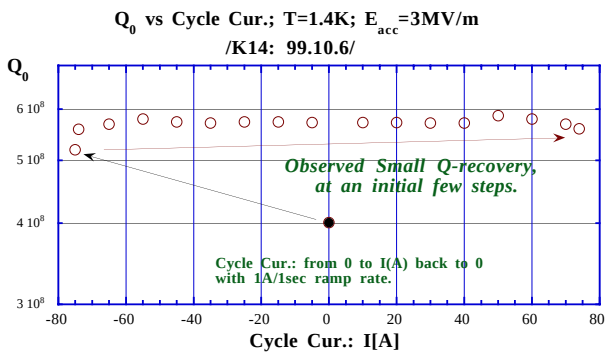

Figure 9: Effects of alternate direction H-field

For each temperature, the sharp Q-drop is observed at the critical H-field, at which the magnetic fluxes might penetrate into the superconducting state and these increase the surface resistance significantly. We call these critical H-fields as a "penetration H-field (H_{pnt})". Once the penetration was occurred, degraded Q_0 was never recovered by simply eliminating the external H-field.

The steep Q-degradation responding to the 1A coil current increasing at H_{pnt} was observed; for example, at T=2.7K, $H_{pnt} \approx$ 935Oe and ΔH_{ext} = 13.75Oe increasing (corresponding 1A increasing) leads to quite small Q_0.

Figure 9 shows the effects of the alternate direction H-field on the cavity at that the fluxes were already penetrated and trapped. The abscissa (cycle cur.) indicate the peak current of one cycle excitation; starting from 0A to peak current and go back to 0A with ramp rate of 1A/1sec. The datum at 0A (black circle) is starting point corresponding to the degraded Q_0 state generated at the initial positive polarity current (corresponding to H_{pnt}). The data of white circle were measured at no external H-field (0A) after at each cycle excitation, and the polarity of one cycle was alternately changed with decreasing the peak current. At an initial few cycles corresponding to the near current of H_{pnt} in absolute, small Q_0-improvements were observed. But almost no Q_0-improvements were observed at a few ampere decreased points in absolute value from the penetration current. These behaviors may suggest a mechanism of flux cancellation in the superconducting state, and will be discussed in later subsection.

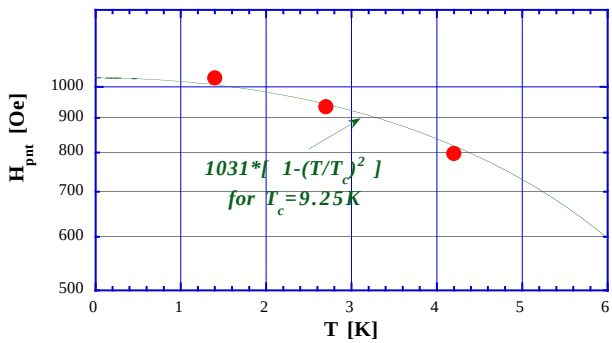

Figure 10: Temperature dependence of penetration H-field

The H_{pnt} versus temperature is shown in Figure 10 with comparison to the empirical temperature dependence of equation (1). The temperature dependence of H_{pnt} is quite consistent with this dependence with the value of $H_{pnt}(0) \approx$ 1030 Oe. This value is almost factor 2 smaller than the thermodynamically defined critical field of niobium ($H_c(0)$ = 2060 ± 50 Oe). The comparison with the value of H_{c1} will also be discussed later.

4.3 Discussion

According to the nature of the niobium, the superconducting state of it is classified to type-II/1 superconductor; the Ginzburg-Landau parameter $\sqrt{2}k$ is greater than 1 but near to 1. The magnetic properties of this type exhibit both behaviors of type-I and type-II such as shown in the magnetization (M) curve as a function of external magnetic field. The schematic behavior is shown in figure 11. Where n is demagnetization coefficient of the sample, and its value is determined by the sample shape directed to the external H-field; for a sphere sample n=1/3. The discussion with using n can be applicable for type-I or type-II/1 at no flux penetration conditions. For type-II with large κ(>>1) the penetration start at quite low

field, therefore the perfect demagnetization is expected only at weak H-field region.

If the cavity made of niobium sheet shows the similar behavior of the bulk niobium sample in the magnetic field, the fluxes penetration start at a reduced critical field (H_{pnt}) that will be defined as,

$$H_{pnt} = H_{c1} \times (1 - n_{eff}) \qquad (7)$$

where n_{eff} is demagnetization coefficient of the cavity, and its effective value will be determined by the shape of the cavity, especially the shape near the equator for our H-filed configuration; the condensation of the field (magnetic flux) is occurred at the equator as shown in figure 7. If we assume $H_{c1}(0) \approx 1700$Oe as discussed in the subsection 2.1 and the temperature dependence of (1) for $H_{c1}(T)$, then the n_{eff} can be estimated as 0.37, 0.40 and 0.41 for T = 1.4, 2.7 and 4.2K, respectively. The obtained n_{eff}'s are consistent with the simulated value of n_{sim} = 0.39, and these are very close to the value of the sphere; 1/3. The cavity cross-section is almost half circle at the equator in a beam axis contained plane, so it will be natural that the n's are almost coincidence with 1/3. If we take the value of $H_{c1}(0) \approx 1800$Oe instead, then n_{eff} are 0.41, 0.43 and 0.44 for these temperature, respectively.

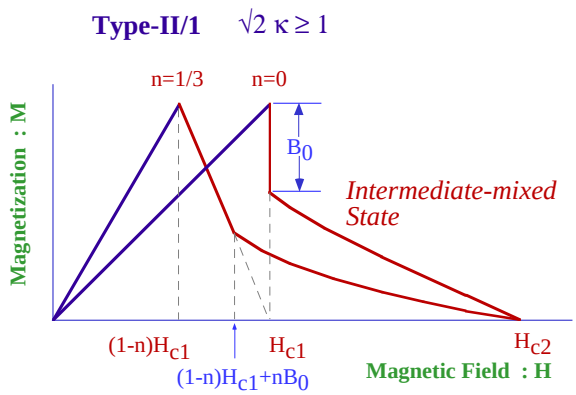

Figure 11: Magnetic properties of Type-II/1 superconductor

The consistency with the n_{sim} is not better than the before, but the accuracy of our analysis can't exclude this possibility.

An area of flux penetration at the H_{pnt} may be estimated from the Q-drop and the applied H_{pnt}, if $R_{mag} = 0.443 \times H_{pnt}$ is assumed. The surface resistance increase at each temperatures are ΔR_s = 413.5nΩ, 311.6nΩ and 1567nΩ, and R_{mag} = 456μΩ, 405μΩ and 353.3μΩ, respectively. The ratio $\Delta R_s / R_{mag}$ will give the percentage of the penetration area. The resultant areas are 54 mm^2, 46 mm^2 and 266 mm^2 for T=1.4, 2.7 and 4.2K, respectively. The procedure described here is used at the later subsection 5.2 to discuss the quench area, and it's justification is also given there. Very thin width belt of the penetration area seems to be produced, if a homogeneous distribution is assumed.

As observed in the previous subsection, only small part of the trapped fluxes could be canceled by the reverse direction external fluxes with almost the same strength magnetic field of H_{pnt}. This fact may indicate the cancellation mechanism. A possible explanation may be such that only the fluxes positioned at the edge are canceled with anti-parallel fluxes that are just begin to penetrate. If we assume the repulsive force for parallel and attractive for anti-parallel flux, there will be always trapped fluxes at the edge in some equilibrium density that is determined by the repulsive force between the trapped fluxes. The attractive force acted between the external anti-parallel and the trapped fluxes may decrease the barrier potential that hinder the penetration of the external fluxes, then even though at the H-field a little lower than the H_{pnt}, the anti-parallel fluxes can penetrate and cancel out the trapped fluxes.

The above discussions assume that the penetrated fluxes could be moved freely in the superconductor. Then the existence of the anti-parallel fluxes can cause perfect cancellation in principle. But the pinning effect is a postulated assumption if we adopted the vortex line as the flux structure (as already adopted in "weak magnetic field"). In this situation, the perfect cancellation can not be expected any more, because two anti-parallel vortexes can not move when the pinning force is stronger than the attractive force; force between the vortexes is function of their distance. Any way, the simple existence of anti-parallel fluxes for the trapped vortex especially for the vortex positioned at far from the edge, can not cause the cancellation.

The consideration given here are applied to rf-case and used in subsection 2.2 to extract H_{c1} value (1800Oe at 0K) from the 40MV/m E_{acc} cavity. A little more (speculative) discussion is given here for the rf-case. If the trapped vortexes can survive for one rf-cycle, in the next parallel phase these may be pushed into interior region by the pressure of H_{ext} and/or by the repulsive force of newly penetrate vortexes. The probability to cancel out at the following anti-parallel phases will be further decreased. In order to get finite probability to survive, some excess field strength might be required if compared to the static field. If we simply take the two values as H_{c1} of 1700Oe (as static case) and 1800Oe (as rf case), then the enhancement factor for rf-case is ~6%.

The next discussions are concerning about the H_{c3} and H_{sh} for rf-case. In the subsection 2.2, we assume the demagnetization coefficient for rf-case is zero (n_{rf}=0). If so, it seems that the H_{c3} must be also taking into account for the critical field consideration. But the thickness of surface superconducting state is only order of ξ (≈38nm for niobium) and this is comparable to the penetration length λ. Therefore, H_{c3} may not contribute to push up the available maximum E_{acc}. It also seems quite difficult to realize any irregularities free surface in the practical

cavity at the order of ξ size. Any irregularity (such as defects, dust, etc.) greater than ξ may destroy the surface super state at least at these places, and flux penetration may occur if H_{rf} is greater than H_{c1}. If the H_{sh} is responsible for available maximum E_{acc} (if another limitations are discarded), our estimated parameters indicate the maximum $E_{acc} \approx$ 53-57MV/m. But the similar discussions may be possible for superheating critical field H_{sh} because that both states are corresponding to the metastable Meissner state at $H_{sh,c3} > H_{ext} > H_{c,c2}$. And the very thin surface area (~λ for this case) is responsible for persistence the superheating state. For the CW operation of the cavity, even though the slow formation speed of nucleation of flux penetration [7], the quench will be induced (at $H_{sh,c3} > H_{ext} > H_{c,c2}$) if the trapped fluxes will remain for one rf-cycle and accumulate these as we discussed before. At non-ideal surface conditions at least at thin surface region (~ξ, ~λ), the bulk properties such as H_{c1} may decided the maximum E_{acc}.

5 QUENCH AT APPLIED FIELD

The (thermal) quench in the superconducting cavity might be inevitable accident if the surface condition is changed. It is also expected that the flux trapping might be happened at the quenched area if the cavity is operated in the applied H-field. The data obtained at the medium strength of H-field are analyzed in this point of view.

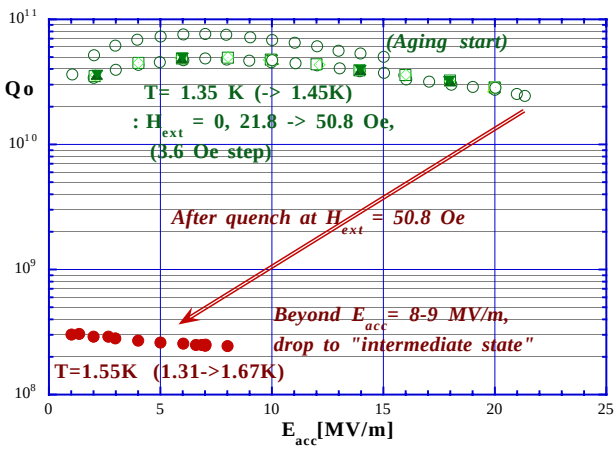

Figure 12: Quench at the medium applied H-field. The Q-E curve at initial and after degradation

5.1 Experiment and Result

At the initial stage of the high field experiments, the applied field were generated by a normal copper wire solenoid coil wound at the out side the cryostat. The available fields were limited to relatively lower field (~50Oe) compared to H_c, because of many troubles in excitation of the coil. After these experiences, we decided to use the superconducting solenoid coil as described in section 4. In the configuration of copper coil, only the outer magnetic shield was used because that the inner shield is set inside the coil (inside the cryostat). The sizable extra magnetization in the outer shield was not observed (at most 1nΩ up in R_{res}, if it were) after 50Oe excitation, but was observed later in 500Oe excitation as discussed in subsection 4.1.

Figure 12 shows the Q-E curve taken at the applied H-fields in the range 0-50Oe, and at 50Oe the thermal quench was initiated. Again the cavity didn't show its best performances, but it may not be relevant to the magnetic characteristics what we want to explore; Q_0 at low E_{acc} is good enough to discuss.

The upper data show the initial Q-E data and the aging to increase the E_{acc} were tried from E_{acc}~15MV/m more than 100 times to reach ~21MV/m. A little degraded Q-values were finally obtained; in the final Q-E curve further degradation were no more observed by the quench. Therefore the effect caused by the quench to degrade the Q-values as reported in reference [8], are not considered in the following analysis. After the quench in the external H-field, the Q_0 were quite degraded. Never recover to the initial Q_0 by the simple elimination of the applied H-field, as similar to the phenomena observed at H_{pnt} in section 4. The Q-E curve at degraded state was also shown. Beyond the maximum E_{acc}(8-9MV/m), the Q_0 were further degraded. But this further degradation was recovered by simply reducing the input power (reducing a dissipation power at the quench area). We usually call this state as "intermediate state" (just as meaning that the state being between the two extreme states) and this state may be interpreted as the thermally equilibrium state between the power dissipation and cooling power. Therefore, don't identify it with the "intermediate state" of type-I or "intermediate-mixed state" of type-II/1 superconductor. Even though, in this case, the (thermal) intermediate state may be caused by the intermediate-mixed state of niobium (see fig.11) as discussed in the next subsection.

5.2 Discussion

The state of the thermal quench induced will be discussed. As the similarities to the states at H_{pnt} in the previous section, the fluxes trapping might be happened. The surface resistance became R_s'= 982nΩ (Q_0= 2.71×10^8 at E_{acc}= 4MV/m) at degraded state. If the quench area is(are) not far from the equator, the size of it may be estimated as follows. Let's take $R_{mag}= 0.433\times H_{ext}$ = 22μΩ for H_{ext} = 50.8Oe and equate R_s' to εR_{mag}, where ε is a percentage of the quench area to the whole cavity area. An obtained radius (if circle is assumed) is 2.9 cm (ε≈4.5% for 600cm^2 cavity area). It seems that this size is consistent with typical temperature map data (for example, shown in [3]), and the estimated value from decay data at the quench with the value of R_n(1-2mΩ) [10]. It was already observed at this experiment that the simple existence of reverse polarity applied H-field didn't improve the degraded state as the same as pointed out at section 4.

The discussion described above indicate that the resultant state is the flux trapped state (intermediate-mixed state) and it's size is consistent with the area of thermal quench. One question may arise concerning about a formation of the flux-trapped state. Because only a simple formation of normal area does not necessarily imply the flux penetration of this area, owing to the hindering current rounded this area in the perfect conductivity (superconducting) region, as explained in the comment given at subsection 4.1. Where the applied H-field (applied afterward the transition with adiabatic condition) can never penetrate the beam pipe tube. Does the transition phenomena of the quench proceed so fast, or any other mechanisms work to trap the fluxes? The formation speed of the quench area seems ~200μs (see the brief comments given in the term of reference [10]), and it seems that this time is long enough to maintain the adiabatic.

A crude (but it may be possible) mechanism is postulated as follow. Let's consider the edge of the hole produced by the quench. Then the large demagnetization coefficient $n_{qch}(\leq 1)$ may be expected at the edge area, if the hole surface is almost perpendicular to the H-field. Sharpness of the edge might be also expected, because of the temperature difference between the inner and outer surface. As a result of large n_{qch} the fluxes penetrate into the super-sate and are trapped at the edge area as the vortex structure. If the above n_{qch} is not large enough by any means, however still the edge area is best place to initiate the flux trapping, because of the T-dependence of H_{c1}; at the edge $H_{c1} \approx 0$ because of $T \approx T_c$. The quench hole might expand to the thermal equilibrium size, then it's size shrink back to zero when rf-energy is dissipated and the quench area is cooled down; it takes ~200μs for former expanding and much longer time for keeping the quenched area as shown in [10]. In the later shrinkage phase, the fluxes trapping are completed for the whole quenched area with increasing a hardness against destruction of the vortexes, because that the n_{qch} becomes small owing to the disappearance of the hole and the H_{c1} becomes large due to the temperature decreasing.

The crudeness of these arguments is the existence of the fluxes in the quench area at the normal state, even though the static penetration of the flux is forbidden as discussed before. Is it possible to penetrate just in the limited region at the near of the normal surface? If so, the flux trapping at the edge may happen and these become hard (energized) to form the static penetration through the cavity when the temperature at the quench area is decreasing. In this case, the exit place may be the beam tube from the energy consumption argument.

The thermocurrent effect is discussed in reference [8] in conjunction with the Q-degradation caused by the quench. And experiments of Nb/Cu clad cavity may confirm this effect [9]. The first Q-degradation may be explained by this effect, but the trapping mechanism of the external field may not be explained. Because the quantity of the flux trapping seems to be decided by the external field itself.

6 SUMMARY

Summarize what we discussed;

- Estimate H_{c1}, H_{c2}.
- Beforehand applied H-field effects on R_{res} , and the temperature dependence of the slope parameter (and T-dependence of R_{res} if origin of it is flux trapping) are discussed.
- Critical H-fields of the cavity were explored experimentally. The magnitude and T-dependence of these indicate that the observed phenomena can be understandable by the H_{c1} and the demagnetization coefficient of the cavity.
- Field trapping at the quench are discussed. Estimates quench size and postulate that the area is intermediate-mixed state. But the question about its formation is unresolved, even though the crude mechanism is tried to explain it.

The topical subjects relevant at each section are discussed. But also, the basic questions concerning for the cavity applications are always in our mind; the origin of the residual resistance and the attainable maximum accelerating field. It seems that the bulk property of niobium such as H_{c1} decided the present achievable E_{acc}=40mV/m in the CW operation.

7 ACKNOWLEDGMENT

The authors would like to thank to the peoples who support these experiments in our laboratories. They express thanks to the members of "PRISM [1]" group, especially to Dr. Y.Kuno, Dr. S.Sakamoto, Dr. K.Shimomura and Dr. S.Sawada of KEK for their help and support. Their gratitude is also expressed to Dr. Y.Iwashita of Kyoto Univ. for his timely and quickly simulations of magnetic field. The cavity was carefully prepared at Nomura Plating Co., Ltd.

8 REFERENCES

[1] Proc. of workshop on "High Intensity Secondary Beam with Phase Rotation", Sep. 21-22, 1998, Nuclear Science Research Facility, Insti. for Chemical Research, Kyoto Univ. Japan

[2] R. P. Huebener, "Magnetic Flux Structures in Superconductors", ISBN 3-540-09213-7 Springer-Verlag.

[3] M. Ono, et al., "Achievement of 40 MV/m Accelerating Field in L-band SCC at KEK", Proc. of 8th Workshop on RF SC, p472, Padova, Italy, 1997

[4] H. Padamsee et al., “Frontiers of Accelerator Technology”, Proc. of the Joint US-CERN-Japan International School on Particle Accelerator, Maui, Hawaii, USA, 1994

C. Benvenuti, et al., “Magnetic Flux Trapping in Superconducting Niobium”, Proc. of 8th Workshop on RF SC, p331, Padova, Italy, 1997

[5] CRC, “HandBook of Chemistry and Physics”, 74th, 1993-1994

[6] K. Saito et al., “TESLA Activities at KEK”, Proc. of 6th SRF Workshop, p372, CEBAF, Newport News, Virginia, USA, 1993

[7]T. Hays, H. Padamsee, “Measuring the RF Critical Field of Pb, Nb, and Nb_3Sn”, Proc. of 8th Workshop on RF SC, p789, Padova, Italy, 1997

[8]J. Knobloch et. al., “Flux trapping in niobium cavities during breakdown events”, Proc. of 8th Workshop on RF SC, p337, Padova, Italy, 1997

[9] T. Fujino et al., “Promising performance of the Nb/Cu clad seamless superconducting rf cavities”, these proceedings.

[10] M. Ono, ”Surface Resistance of Niobium Cavity”, Proc. of 1st Superconducting Linear Acc. Meeting in Japan, KEK, Japan, 1998. [Contents are written in Japanese, so briefly summarized here about the decay behavior at the quench. Let’s take the values, R_n(at room T) =26m Ω(measured), √RRR(300) =17.3, then R_n(~2K)=1-2 mΩ. Energy conservation imply; dU/dt = P. Dissipation power can be expressed; P =($\varepsilon R_n + (1-\varepsilon)R_s)\times I^2 \approx \varepsilon Rn \times I^2$. And the stored energy; $U=G/\omega \times I^2$. Where I is rf-current, G is geometrical factor of the cavity, and ε is percentage of quench area. Then, $\varepsilon R_n = G/\omega \times (dI/Idt)$. If R_n is given, then ε can be estimated from decay data at time t. The development of the quench area were observed in the actual data; it takes ~200μs to reach to the equilibrium size, as shown in the figures.]

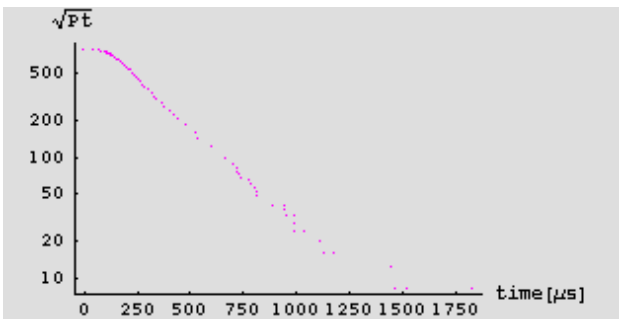

($\sqrt{p_t}$ is the transmitted power, then $\sqrt{p_t} \propto I$)

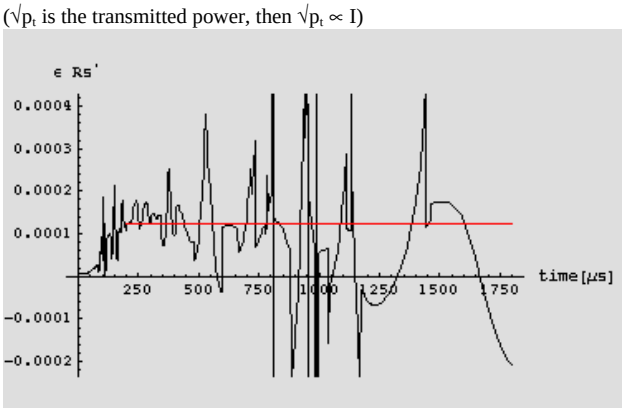

(Quench size at time t; $\varepsilon R_n = G/\omega \times (dI/Idt)$)